J Fluoresc (2014) 24:695–707
DOI 10.1007/s10895-013-1340-5

ORIGINAL PAPER

Spectral and Molecular Modeling Studies on Hydroxybenzaldehydes with Native and Modified Cyclodextrins

M. Jude Jenita · T. Mohandass · N. Rajendiran

Received: 16 September 2013 / Accepted: 27 November 2013 / Published online: 6 December 2013

Abstract The inclusion complexation of 2-hydroxy-3-methoxybenzaldehyde (2HMB), 4-hydroxy-3-methoxybenzaldehyde (4HMB), 3,4-dimethoxybenzaldehyde (DMB) and 4-hydroxy-3,5-dimethoxybenzaldehyde (HDMB) with α-CD, β-CD, HP-α-CD and HP-β-CD were carried out by UV-Visible, steady-state and time-resolved fluorescence and PM3 methods. All the benzaldehydes shows dual fluorescence in aqueous and CD mediums and 1:1 inclusion complexes were formed with CDs. PM3 geometry optimizations results indicate that the HDMB/CD complex is significantly more favorable than the other complexes. The negative enthalpy changes suggest that the inclusion complexation processes are spontaneous. The geometry of the most stable complex shows that methoxy/OH group of HMBs is entrapped in the less polar CD cavities, while the aldehyde group present in the upper part of the CDs cavities.

Keywords Aldehydes · Cyclodextrin · Inclusion complex · Intramolecular charge transfer · Molecular modeling · Fluorescence

Introduction

α-, β-, γ-Cyclodextrins (CDs) are cyclic oligomers of six, seven and eight α-d-glucose units connected through glycosidic α-1,4 bonds [1]. These compounds, usually characterized as a doughnut or wreath-shaped truncated cones, have a hydrophobic cavity of appropriate dimensions and hence can form inclusion complexes with a variety of organic compounds in the aqueous solution [2]. Model studies on CD complexation offer valuable insights into molecular recognition and enzyme–substrate interactions [3]. In addition to experimental approaches, theoretical calculations [4] can illustrate the driving forces of the complexation [5] and the inclusion regioselectivity in CD-catalyzed reactions [6]. Due to the large size, most calculations on CD chose the molecular mechanic (MM) method based on various empirical force fields [7–10]. However, as MM method has difficulty in modeling the molecules in their excited states, quantum mechanics (QM) methods must also be developed to study the CD chemistry [11–13].

Investigation and application of cyclodextrins (CDs) and their inclusion complexes in food, cosmetic and pharmaceutical industries as well as in separation technologies has greatly increased in the last decades [14–16]. They are nontoxic and safe to use as encapsulating materials for drugs and biologically active compounds. Availability of a relatively non-polar internal cavity in the toroidal structure of CD brings about the inclusion complex formation of CDs with various organic molecules. The properties (solubility, stability, test, activity) of guest molecules placed inside the CD cavity can be significantly changed. Thus, the practical importance of CDs inclusion complexes is evident.

Our earlier studies on 4-hydroxy methoxybenzaldehydes [17, 18], 4-hydroxy methoxybenzoic acids [19, 20] and hydroxy methoxybenzoic acids [21, 22] clearly shown that the formation of ICT state in polar solvents and β-CD. In fact it has been established that the barrier height for the ICT process decreases with the increase in the solvent polarity. In this paper, the effect of α-CD, β-CD, HP-α-CD and HP-β-CD on the absorption and fluorescence spectra of 2-hydroxy-3-methoxy benzaldehyde (2HMB, *ortho* vanillin), 4-hydroxy-3-methoxy benzaldehyde (4HMB, vanillin), 3,4-dimethoxy

Electronic supplementary material The online version of this article (doi:10.1007/s10895-013-1340-5) contains supplementary material, which is available to authorized users.

M. J. Jenita · T. Mohandass · N. Rajendiran (✉)
Department of Chemistry, Annamalai University, Annamalai nagar 608 002, Tamilnadu, India
e-mail: drrajendiran@rediffmail.com

benzaldehyde (DMB, veratraldehyde) and 4-hydroxy-3,5-dimethoxy benzaldehyde (HDMB, syringaldehyde) were studied. The inclusion complexes of these benzaldehydes with α-CD, β-CD, HP-α-CD and HP-β-CD were investigated by UV-visible, steady state fluorescence, time resolved fluorescence and molecular modeling methods. The complexation energies of the above mentioned molecules and CD during the formation of inclusion complexes were studied using PM3 method in the aim to give some insights about the location of hydroxyl group of the guest molecules toward primary or secondary hydroxyl of CD. We also determine the driving intermolecular interactions during the formation of such complexes with the following points, (i) whether the encapsulation of the hydroxyl groups same or different and (ii) the intramolecular charge transfer effect of these molecules in CD media to affect the complexation energy and intermolecular interactions.

Experimental

Reagents and Methods

All the aldehydes and CDs were obtained from Sigma-Aldrich and used as such. Solutions in the pH range 2.5–12.0 were prepared by adding appropriate amount of phosphate buffer (NaOH and H_3PO_4). A modified Hammett's acidity scale (H_0) [23] for the solutions below pH ~2 (using a H_2SO_4-H_2O mixture) and Yagil's basicity scale (H_-) [24] for solutions above pH ~12 (using a NaOH-H_2O mixture) were employed. Triply distilled water was used for the preparation of aqueous solutions. The solutions were prepared just before taking measurements. The concentration of the drug solutions were in the order of 4×10^{-4} to 4×10^{-5} M. The concentrations of CDs were varied from 1×10^{-3} to 10×10^{-3} M. The experiments were carried out at room temperature 303 K.

Instruments

Absorption spectral measurements were carried out with a Shimadzu UV-Visible spectrophotometer (model 1650 PC) and fluorescence measurements were made by using a Shimadzu spectrofluorimeter (model RF-5301). The pH values in the range 2.5–12.0 were measured on an Elico pH meter (model LI-120). The fluorescence lifetime measurements were performed using a picoseconds laser and single photon counting setup from Jobin-Vyon IBH.

Molecular Modeling

The theoretical calculations were performed with Gaussian 03 W package. The initial geometry of the HBs, α-CD and β-CD were constructed with Spartan 08 and then optimized by PM3 (Parametric method 3). Both CDs were fully optimized by PM3 without any symmetry constraint [25–27]. The glycosidic oxygen atoms of CD were placed onto the XY plane and their centre was defined as the centre of the coordination system. The primary hydroxyl groups were placed pointing toward the positive Z axis. The inclusion complexes were constructed from the PM3-optimized the CD and the guest molecules. The longer dimension of the guest molecule was initially placed onto the Z axis. The position of the guest was determined by the Z coordinate of one selected atom of the guest. The inclusion process was simulated by putting the guest in one end of CD and then letting it pass through the CD cavity. Since Density Functional Theory (DFT) calculations are expensive (cost and takes long time) in treating such large molecular systems, we used single point energy calculations to the PM3 optimized geometries using semiempirical method as implemented in Gaussian 03 W [25–28].

Results and Discussion

Effect of Cyclodextrins

Figures 1, 2 and supporting Figures S1 and S2 depict the absorption and emission spectra of 2HMB, 4HMB, DMB and HDMB (2×10^{-5} M) in pH ~7 solutions containing different concentrations of α-CD, β-CD HP-α-CD and HP-β-CD. We provided the spectra of α-CD and β-CD only, because the spectral shapes and shifts of the aldehydes with HP-α-CD and HP-β-CD inclusion complexes were similar to the α-CD and β-CD inclusion complexes respectively. The absorption maxima of all the above benzaldehydes in water (2HMB: λ_{abs} ~342, 310, 264, 217 nm, λ_{flu} ~338, 500 nm; 4HMB: λ_{abs} ~311, 279, 231 nm, λ_{flu} ~329, 425 nm; DMB: λ_{abs} ~307, 277, 230 nm, λ_{flu} ~335, 433 nm and HDMB: λ_{abs} ~304, 213 nm, λ_{flu} ~330, 434 nm) were red shifted than that of 4-hydroxy benzaldehyde (HB: λ_{abs} ~294, 221 nm).

With on increasing the four CDs concentrations, the above benzaldehydes have not shown any significant spectral shifts in the absorption spectra. However, the absorbance of all the aldehyde molecules regularly increased along with the CDs concentrations. The changes in the absorbance and fluorescence intensities of the above benzaldehydes measured as a function of α-CD, β-CD, HP-α-CD and HP-β-CD were plotted in the inset (Figs. 1, 2, 3 and 4). A similar trend was also observed in pH ~1 solutions. In the absorption spectra, the presence of isosbestic point in all the benzaldehydes indicates the possibility of a single equilibrium involving 1:1 complexation between the guests and the CDs. The association constants can therefore be evaluated from the Benesi–Hildebrand equation [29, 30] for the 1:1 inclusion complexes of all the CDs with the aldehydes. Figures 3 and 4 show a plot of $1/A\text{-}A_0$ and $1/I\text{-}I_0$ as a function of 1/[CD] and a plot of $1/A\text{-}A_0$ and $1/I\text{-}I_0$ as a function of $1/[CD]^2$. From the intercept and

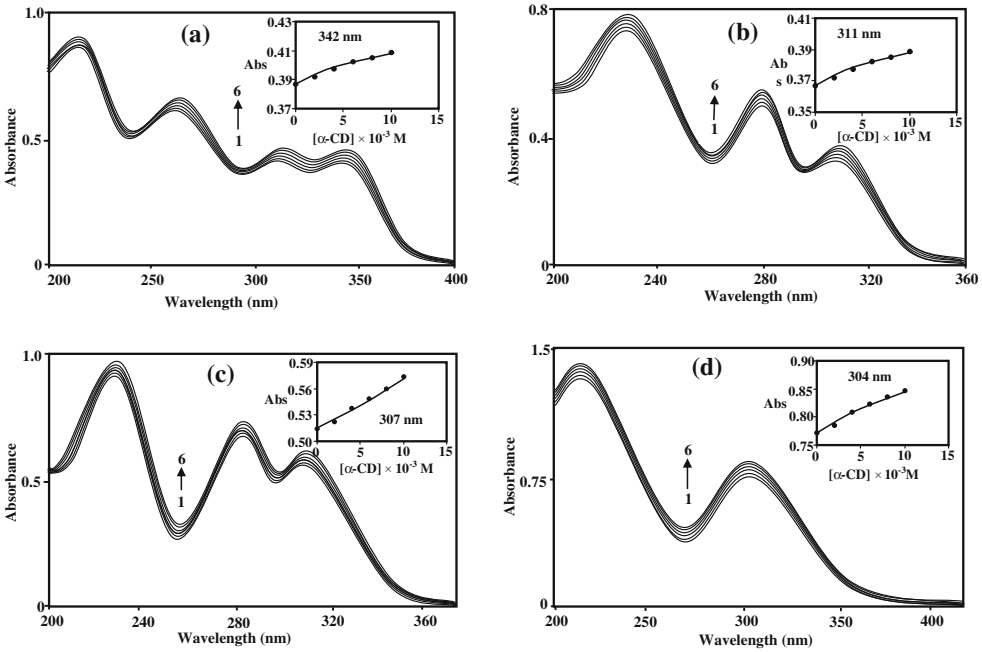

Fig. 1 Absorption spectra of **a** 2HMB, **b** 4HMB, **c** DMB and **d** HDMB in different α-CD concentrations (M) at pH ~7: (1) 0, (2) 0.002, (3) 0.004, (4) 0.006, (5) 0.008 and (6) 0.01. Insert Fig.: absorbance vs. α-CD concentrations

slope values of this plot, K values were determined. Good linear correlations were obtained confirming the formation of 1:1 inclusion complexes.

The fluorescence spectra of all the benzaldehydes with α-CD, β-CD, HP-α-CD and HP-β-CD are displayed in (Figs. 2 and S2). In the excited state, the above benzaldehydes reflect remarkable changes in all the CD solutions. The above benzaldehydes exhibit a dual fluorescence of locally excited (shorter wavelength, SW) and ICT (longer wavelength, LW) states in water and CD solutions. Absorption and emission maxima of 2HMB are red shifted than that of other aldehydes. In aqueous and CD media, the LW band intensity of 2HMB, 4HMB and HDMB were greater than SW band intensity whereas in DMB, the SW intensity was greater than LW band intensity. With an addition of CDs both SW and LW intensities increases in all the aldehydes. However, in DMB and HDMB the rate of enhancement of the SW emission is greater than that of LW band. In 2HMB and 4HMB, the LW fluorescence intensity is greater than SW band intensity. In CD solutions, the LW and SW band of 4HMB, DMB and HDMB increased

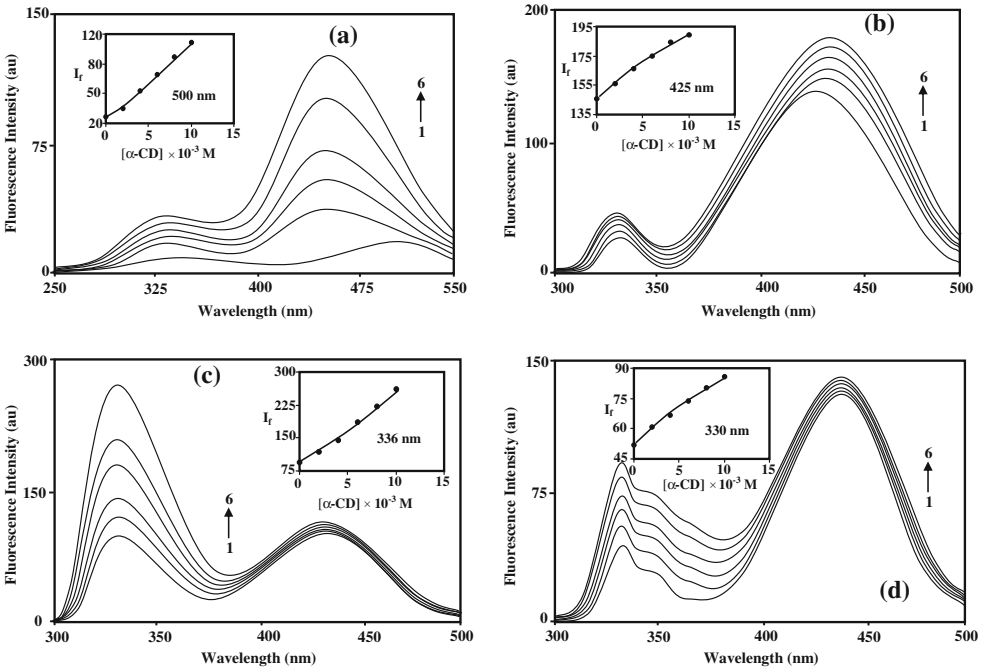

Fig. 2 Fluorescence spectra of **a** 2HMB, **b** 4HMB, **c** DMB and **d** HDMB in different α-CD concentrations (M) at pH ~7: (1) 0, (2) 0.002, (3) 0.004, (4) 0.006, (5) 0.008 and (6) 0.01. Insert Fig.: absorbance vs. α-CD concentrations; Excitation wavelength : **a** 2HMB – 342 nm, **b** 4HMB - 310 nm, **c** DMB – 335 nm, and **d** HDMB – 330 nm

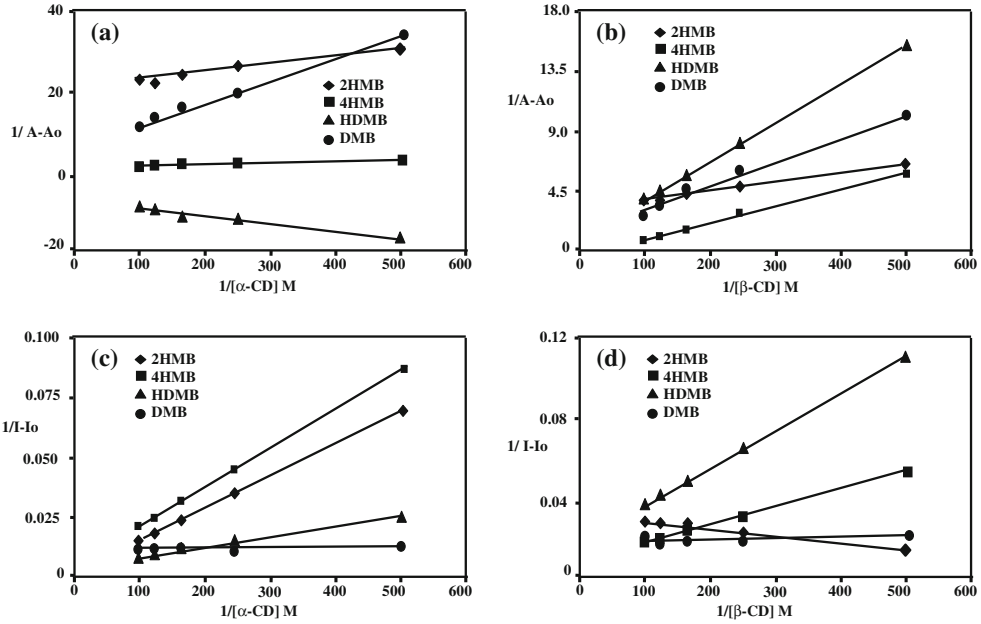

Fig. 3 Benesi-Hildebrand plot for 1:1 inclusion complexation of HMBs with α-CD and β-CD at *p*H ~7: (**a**) and (**b**) plot of 1/A-A_o vs. 1/[CD], (**c**) and (**d**) plot of 1/I-I_o vs. 1/[CD]

at the same wavelength. Interestingly, in 2HMB, with increasing the CDs concentrations, a large blue shift were observed in the LW bands, whereas no significant spectral change were seen in the SW bands. This can be seen more clearly from looking at the (Figs. 2 and S2). The SW band intensities of 2HMB in 0.01 M CD solution is increased to 0.5 times more than that of aqueous medium and LW band emission enhanced approximately 10 times. Further, the fluorescence intensities of LW band increases with increase in the excitation 270 nm to 320 nm. This may be the extended π-conjugation would induce an excited state resonance contribution of the carbonyl group to the benzene ring resulting in the increased polarity to facilitate the interaction with water. The SW fluorescence intensities increased from lower to higher CD concentrations. Further LW band is largely red shifted in more protic solvents than SW band. The above results may assume ICT present in these molecules [22, 30–36]. If the LW band maximum was due to ICT, the intensity of fluorescence may decrease in CD solutions. The presence of LW emission maxima in DMB suggests ICT present in these aldehydes. Further, appearance of LW band in a hydrocarbon solvent indicates that ICT emission associated with H-bonding [17, 18] is present in these aldehydes. The reason for the LW band is already explained in our earlier

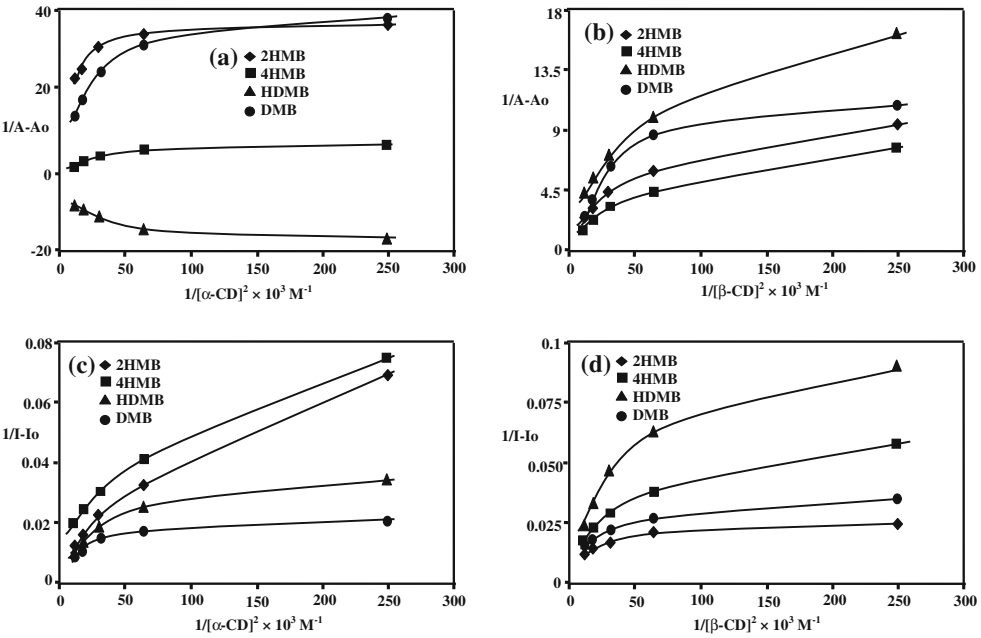

Fig. 4 Benesi-Hildebrand plot for 1:2 inclusion complexation of HMBs with α-CD and β-CD at *p*H ~7: (**a**) and (**b**) plot of 1/A-A_o vs. 1/$[CD]^2$, (**c**) and (**d**) plot of 1/I-I_o vs. 1/$[CD]^2$

publications [19, 20, 31–36]. The LW band fluorescence regularly red shifted from non-polar to polar solvents [19, 20, 35, 36]. The intensity of LW band also increased from cyclohexane to water. Further LW band was largely red shifted more in protic solvents than SW band. The appearance of the LW band in a hydrocarbon solvent indicates that ICT is present in all the aldehydes.

The full width at half the maximum height (FWHM) of the ICT fluorescence band increased with increase in the CD concentrations [17–22]. FWHM of the band ICT fluorescence was different in water and CD solutions. This is because these aldehydes have multi functional groups (OH, CHO, and OCH_3). Hence the emission of a state with a high ICT character is stabilized by H-bonding with the solvent. In such a state, the donor group is the OH/methoxy/aromatic moiety of the aldehydes molecules and the CHO group is the acceptor. Further, the increase of SW fluorescence intensities in DMB and LW fluorescence intensities in other HMBs confirm the above prediction. These results again support that the ICT emission present in all these molecules.

The CD dependent emission spectra show that the ICT band is less sensitive to increase in all the CD concentrations, whereas the SW band shows an enhancement. Inside the CD cavities, HMB feels much less polar environment and the main non-radiative path of the locally excited band (through ICT) is restricted which also causes an enhancement of the SW band. Further, the geometrical restriction of the cavity would prevent the free rotation of the CHO or OCH_3 groups in the CDs cavities and thus hinder the formation of ICT state causing an enhancement of normal SW band.

The binding constant (K) values in α-CDs are greater than β-CDs which indicate that the benzaldehyde molecules are more tightly encapsulated in the α-CDs cavity than β-CDs. The 'K' value of HDMB is less than other HMBs which indicates that 2HMB, 4HMB and DMB are more deeply included in the β-CDs cavities than HDMB. Since the band distance between the two methoxy groups is greater than the CDs cavities size; hence it is partially included in the CDs cavities. Since the band distance of other aldehydes (2HMB/4HMB/DMB) is less than CDs cavities size these molecules may completely encapsulated in the CDs cavities. As can be seen from Table 1, ΔG values are negative which suggest that the inclusion processes are exothermic and spontaneous.

Table 1 show that the binding constants were apparently varied with the properties of the substituents. The substituent with a larger 'K' value fits more tightly into the CDs cavities. Further, the higher polarizability of the substituent's with larger 'K' values favors binding through interaction between permanent dipoles of CDs and induces dipoles of guests. The strength of interaction is also dependent on the size of the CDs cavities. As Figs. 3 and 4 shows the slope of the straight line for α-CD is twice that of β-CD. This means that the interactions are more sensitive to the size of substituents in the complexation of α-CD than β-CD. Further the SW fluorescence intensity higher than LW supports this implication.

Table 1 Absorption, fluorescence, lifetime, binding constant and ΔG values of 2HMB, 4HMB, DMB and HDMB in water and α-CD and β-CD environments

Compound	Medium	λ_{abs} nm	log ε	λ_{flu} nm	<τ> ns	Binding constant (K^{-1})		ΔG k cal mol^{-1}	
						Abs	flu	abs	flu
2HMB	Water	342	3.76	500	1.17				
		310	3.78	338					
		264	4.61						
		217	4.83						
	α-CD	344	3.85	455	2.42	105	183	−2.80	−3.13
		310	3.84	330					
		364	4.57						
		218	4.79						
	β-CD	342	3.95	455	3.68	250	320	−3.32	−3.46
		310	3.94	330					
		263	4.57						
		218	4.79						
4HMB	Water	311	3.56	425	1.49				
		279	4.20	329					
		231	4.36						
	α-CD	312	3.68	429	2.60	163	295	−3.06	−3.42
		280	4.30	330					
		231	4.47						
	β-CD	312	4.00	430	3.06	296	384	−3.42	−3.58
		282	4.07	330					
		231	4.13						
DMB	Water	307	4.20	433	0.68				
		277	4.29	335					
		230	4.44						
	α-CD	307	4.33	435	1.06	98	124	−2.76	−2.90
		277	4.41	337					
		230	4.54						
	β-CD	306	4.43	436	1.42	157	243	−3.04	−3.30
		279	4.36	336					
		232	4.44						
HDMB	Water	304	4.40	434	2.22				
		213	4.52	330					
	α-CD	306	4.52	433	3.71	269	373	−3.36	−3.56
		215	4.65	330					
	β-CD	304	4.70	433	4.25	372	493	−3.56	−3.73
		217	4.80	330					

Several driving forces are possible for the inclusion complexation of CD with guest compounds. However, in these molecules, the hydrogen bonding interactions play a major role in the inclusion complexation of CD with these aldehydes. In these cases, the inclusion process is determined by the aldehyde and hydroxyl groups. The 'K' values are a reasonable measure of hydrogen bonding and the change in hydrogen bonding of aldehydes is caused only by the hydrogen ion concentration. Since the hydroxyl and methoxy substituent locate near the narrower rim of the CD cavity and aldehyde group locates at wider rim of the CD cavity, the 'K' values are proportional to the hydrogen bonding interactions. In DMB, the SW and in other HMBs the LW fluorescence

intensities are greatly enhanced with increasing CD concentrations which support this prediction. The difference in slopes in Figs. 3 and 4 for the inclusion complexes indicates that the interactions of hydrogen atoms, especially with β-CDs are much stronger than α-CDs because HMB interactions are approximate to the hydrogen bonding contact with α-CDs. They are somewhat weak, since the hydroxyl groups are far from the internal surface of the β-CD cavity in the inclusion complexes. Thus for HMB, the binding constant with β-CDs are greater than with α-CDs Table 1.

In order to substantiate this, the absorption and emission maxima of all the aldehydes were measured in different polorities of the solvents (Table 2). Compared to in any one solvent, the absorption and emission maxima of 2HMB was red shifted than that of 4HMB, DMB, HDMB and HB (cyclohexane: λ_{abs} ~288, 281, 274 and 265 nm, methanol: λ_{abs} ~294, 221 nm). The absorption spectra of 2HMB is different from other molecules is due to the greater charge transfer interaction of the aldehyde group with the aromatic moiety and/or hydroxyl group. 2HMB show absorption maxima around 350 nm in nonpolar solvents suggest that intramolecular hydrogen bonding (IHB) present in this molecule. The molar extinction coefficient is very high (~10^{-4} cm^{-1}) and the absorption maximum slightly blue shifted from 350 nm to 340 nm as the solvent polarity increases imply that this IHB band was affected by the polar solvents. The absorption maxima of DMB and HDMB were red shifted than 4HMB indicates, addition of methoxy groups in HB molecules increasing the interaction between hydroxy and aldehyde groups.

The LW band fluorescence were regularly red shifted from non polar to polar solvents (Table 2). The intensity of LW band was also increases from cyclohexane to water. It should also be pointed out, the fluorescence intensity of the LW band increases with increase in the λ_{exc} ~280 to 320 nm. Further LW band was largely red shifted in more protic solvents (350 to 430 nm) than SW band (323 to 335 nm). The appearance of the LW band in a hydrocarbon solvent indicates that intramolecular charge transfer (ICT) present in all these aldehydes.

The SW band fluorescence intensities increased from lower to higher CD concentrations. The above results may assume different species present in these molecules. The presence of LW emission maxima in DMB suggests ICT present in all these aldehydes. The appearance of the LW band in a hydrocarbon solvent indicates that ICT emission associated with H-bonding [17, 18] present in these molecule. Supporting this implication the excitation spectra exhibit the monitoring wavelength dependence. The excitation spectrum for the 430 nm fluorescence was distinctly different from that for the 330 nm fluorescence. Further, the fluorescence spectrum in the water solution was significantly changed on addition of dioxane showing a dual emission and an isoemissive point in water-dioxane mixture. As expected [17, 18] the fluorescence maximum of band LW red shifted with an increase of methanol content. The ICT emission increases in protic solvents suggesting that the hydrogen bonding interactions plays a

Table 2 Absorption and fluorescence spectral data (nm) observed for 2HMB, 4HMB, DMB and HDMB in different solvents

Solvents	2HMB		4HMB		DMB		HDMB	
	λ_{abs}	λ_{flu}	λ_{abs}	λ_{flu}	λ_{abs}	λ_{flu}	λ_{abs}	λ_{flu}
Cyclohexane	340	400 s	295	348	298	350	300	325
	264	320	270	323	270	321	288	
	219		232		227		226	
							217	
1,4-Dioxane	340	440	305	357	306	368	309	337
	264	325	273	328	273	325	230	
	219		231		228			
Acetonitrile	340	445	304	359	309	405	310	340
	264	325	272	323	278	327	228	390 s
	219		231		228			
2-Propanol	342	464	311	382	308	412	310	330 s
	264	325	281	326	279	328	231	400
	218		235		228		216	
Methanol	342	470	308	393	306	414	308	330
	262	325	279	327	278	329	254	410
	218		234		228		215	
Water(pH ~6.5)	340	490	290	425	306	430	300	330
	260	326 s	256	327	279	335	217	430
	218		218		228			

major role in the ICT emission. The dual emission observed in DMB support the presence of ICT in these aldehydes, because monocation formation is not possible in these aldehydes.

From the above results, it is clear that in CD solutions, the surrounding polarity of aldehyde groups does not change very much as there is no hypsochromic shift of the most polar (ICT) state [37, 38] of aldehydes, but the relative intensity (I_{ICT}/I_{LE}) increases with the increase of CDs concentration. This may only be possible if the orientation of these molecules is such that the aromatic ring goes inside the CDs cavities and the aldehyde group is present in the upper part of the CDs cavities. Further, if aldehyde group is present in the inner CDs cavities, a hypsochromic shift or absence of ICT emission could be observed in the CD medium. However, a large hypsochromic shifts observed in 2HMB indicates that this molecule is completely encapsulated in the CDs cavities. This is because the size of this molecule is smaller than CDs cavities. Further, the emission enhancement in α-CDs solution is higher than β-CDs, which reveals that, the smaller sized α-CDs cavities restrict the free rotation of the benzaldehyde molecules.

Effect of Acid/Base Concentrations

Further, the effect of CD on the prototropic equilibrium between neutral, monoanion on the pH dependent changes in the absorption and emission spectra of these molecules in CD solution were measured. The spectral data of the prototropic species of all the aldehyde molecules is complied in Table 3. With an increase in pH from 7 to 10, a red shift is observed in the absorption spectrum and this reflects the formation of the monoanion. The proton can be removed from the hydroxyl group because the pK_a value for this reaction is 10, calculated spectrophotometrically and it's agreement with the value for the deprotonation reaction of the OH group of all the aldehyde molecules. A similar pK_a value is observed in the case of all the aldehyde molecules further confirmed deprotonation takes place in the hydroxyl group. When the hydrogen ion concentration is increased from pH ~7 to 1, a red shift is noted in the absorption spectra indicates that, the monocation species formed by protonating the carbonyl group. The above assignments are consistent with the earlier finding shows that, the red shift in the absorption when protonation takes place at the carbonyl group or when deprotonation takes place from the hydroxyl group [17–22].

The changes observed in the fluorescence spectra of all the aldehyde molecules follow the same trend as that observed in the corresponding reactions ground state. The absorption and emission maxima were studied in 6×10^{-3} M CD solutions in the pH range 0.1 to 11.0. When compared to aqueous medium, a slight blue shift were observed in the absorption maxima of neutral, whereas a large blue shift was observed in the monoanion maxima of the benzaldehydes in CD medium than aqueous medium. These results again supported OH group of

Table 3 Various prototropic maxima (absorption and fluorescence) of 2HMB, 4HMB, DMB and HDMB in aqueous, α-CD and β-CD medium

		Aqueous		α-CD		β-CD	
		λ_{abs}	λ_{flu}	λ_{abs}	λ_{flu}	λ_{abs}	λ_{flu}
2HMB	Monocation	344	496	337	481	338	482
		267	300	263	320	263	319
		224		215		215	
	Neutral	340	468	342	455	342	468
		265	324	263	300	256	332
		220		217		222	
	Monoanion	395	550	386	517	390	459
		281	353	281	316	275	319
		235		236		235	
4HMB	Monocation	292	358	290	351	290	348
		259	400	259		259	
		218		220		220	
	Neutral	289	426	312	429	285	425
		256	325	280	330	258	330
		218		231		220	
	Monoanion	299	359	277	415	282	358
		216		218		250	
						217	
DMB	Monocation	310	435				
		283	339				
		228					
	Neutral	308	430	307	432	306	430
		280	336	277	335	277	355
		226		230		227	
HDMB	Monocation	315.4					
		219.0					
	Neutral	300	420-	359	433	298	425
		217	430	306	330	221	330
			330	215			
	Monoanion	371	430	362	420	368	430
		264 s	330	250		256	330
		251		212		218	
		222					

of all the aldehyde molecules were more deeply entrapped in the CD cavities than aldehyde group.

Excited State Singlet Lifetime

In order to confirm the interpretation of the steady-state fluorescence, the time-resolved fluorescence decay times of all the aldehydes in the CDs solutions were investigated. The average fluorescence lifetimes are presented in Table 1. Analyzing the fluorescence decay obtained at different observation, it is found that for monitoring wavelength corresponding to the maximum of SW (330 nm) fluorescence band, there are two

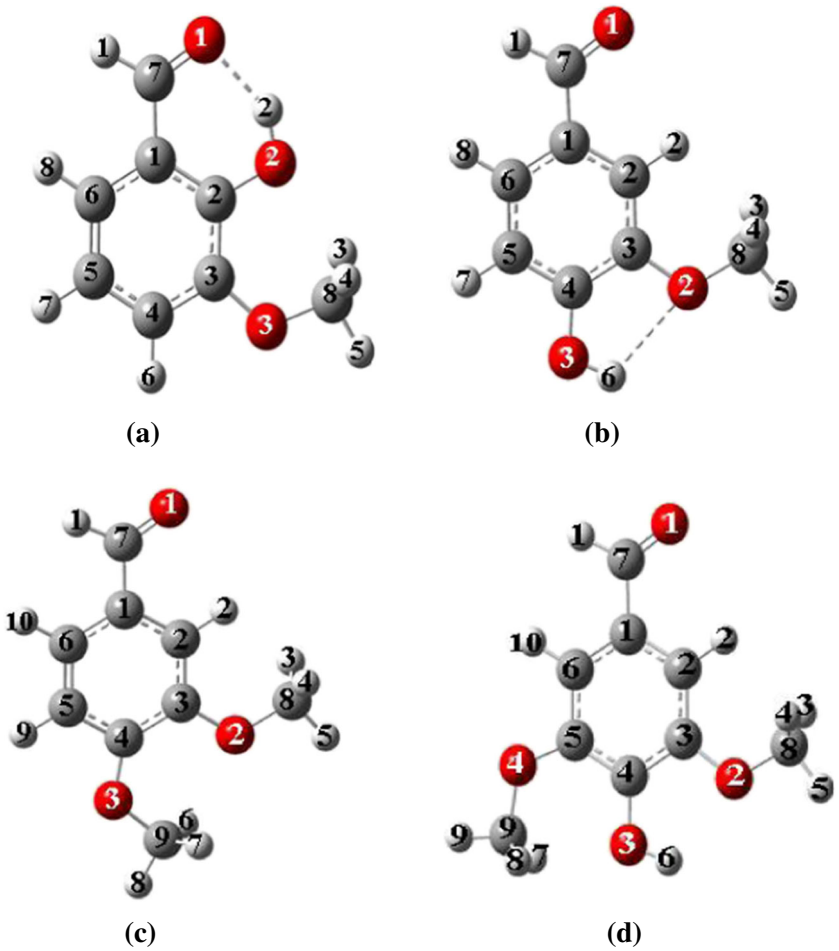

Fig. 5 CAChe – DFT optimized structure of 2HMB, 4HMB, DMB and HDMB

decay components, whereas for LW (430 nm) fluorescence decays are very well fitted by a three-exponential function. On the basis of the performed analyses of the experimental lifetime and pre-exponential factor, we suppose that in aqueous solutions containing different concentrations of CDs, two or three fluorescence emitting centers exist. The CD dependent biexponential decay times of the SW emission lead us to conclude that the fast decay component originates from the emission of the hydrogen bonded complexes, whereas the slow decay component results from 1:1 type inclusion complexes. It is worth to note that the relative amplitude of the 1:1 type inclusion complex emission increases as the CD concentration increases. In all the four CDs, the decay pattern monitored at the LW emission differed considerably from that at SW emission. For a monitoring wavelength corresponding to the maximum of LW fluorescence band, an additional decay component appears in the fluorescence decay.

Solid Inclusion Complex Studies

Further to confirm the HMB:CD interactions, we also prepared the solid inclusion complexes and characterized by FTIR and ^{1}H NMR methods.

FTIR Spectral Studies

(i) **2HMB/4HMB**: The OH stretching vibrations in 2HMB/4HMB produce a strong band in the 3159 cm^{-1} region which is largely red shifted in the inclusion complex to 3397 cm^{-1}. The OH bending at 1305 cm^{-1} and out of plane deformation frequencies at 745 cm^{-1} also red shifted in the inclusion complex to 1381 and 763 cm^{-1}, respectively. The C–O–CH_3 symmetric stretching frequency at 1095 cm^{-1} slightly red shifted in the complex. Further C=C aromatic ring stretching at 1589 cm^{-1} also red shifted in the complex to 1597 cm^{-1}. However, the C=O stretching vibration at 1673 cm^{-1} blue shifted in this complex to 1682 cm^{-1}. Further, the absorption intensity of the inclusion complex is also significantly varied from free guest molecules.

(ii) **DMB**: The OH stretching vibrations in DMB produce a strong band in the 3077 cm^{-1} region which is largely red shifted in the inclusion complex to 3345 cm^{-1} respectively. The OH bending at 1379 cm^{-1} and out of plane deformation at 735 cm^{-1} frequency also red shifted in the inclusion complex to 1394 and 758 cm^{-1}. The C–O–CH3 symmetric stretching frequency at 1036 cm^{-1}

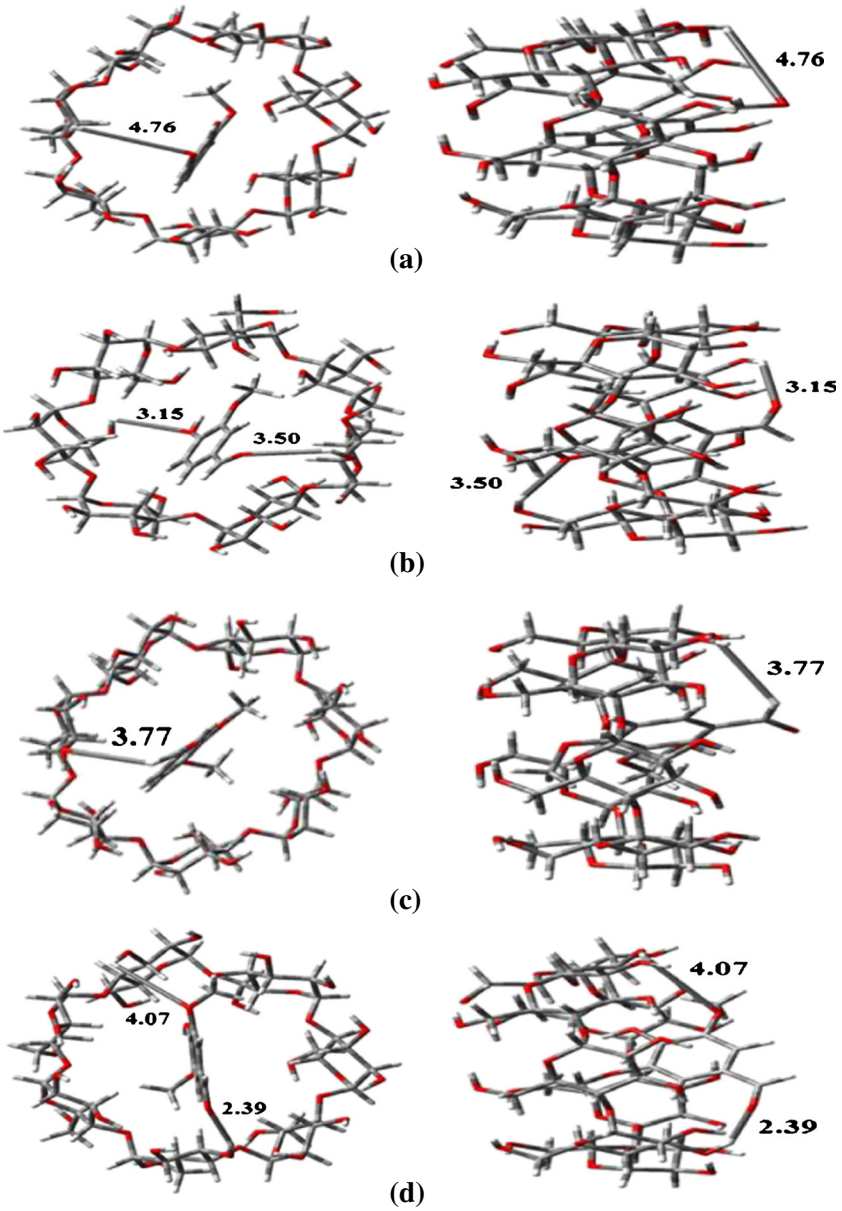

Fig. 6 The proposed inclusion complex structure of 2HMB, 4HMB, DMB and HDMB

slightly red shifted in the complex. Further, C=C aromatic ring stretching at 1598 cm^{-1} also red shifted in the complex to 1608 cm^{-1}. However, the C=O stretching vibration at 1672 cm^{-1} blue shifted in this complex to

Table 4 Binding energies and HOMO, LUMO energy of 2HMB, 4HMB, DMB and HDMB before inclusion complexation by PM3 method

Properties	2HMB	4HMB	DMB	HDMB	α-CD	β-CD
E_{HOMO} (eV)	−8.95	−9.15	−9.02	−9.05	−10.38	−10.35
E_{LUMO} (eV)	−0.68	−0.46	−0.42	−0.46	1.26	1.23
$E_{HOMO} - E_{LUMO}$ (eV)	−8.27	−8.69	−8.60	−8.59	−11.64	−11.58
Dipole Moment(D)	1.68	1.24	1.71	2.16	11.34	12.29
E*	−91.44	−92.48	−81.76	−125.25	−1247.52	−1457.63
G*	20.49	23.44	3.48	38.16	−571.21	−667.55
H*	7.13	5.55	33.29	6.24	−676.73	−789.52
S**	0.092	0.097	0.099	0.107	−0.353	−0.409
Zero point energy	92.35	91.29	108.00	110.99	634.47	740.56

Unit * = $Kcalmol^{-1}$, ** = cal/mol-Kelvin

1681 cm^{-1}. Further, the absorption intensity of the inclusion complex is also significantly varied from free guest molecules.

^{1}HNMR Spectral Studies

Proton NMR (400 MHz in D_2O) was used to compare the environments of the pure and complexed molecules and in particular to confirm interactions of the guest molecules. Proton nuclear magnetic resonance (^{1}H NMR) spectroscopy has proved to be a powerful tool in the study of inclusion complexes [30–33]. The resonance assignment of the protons of CD are well established [13, 14] and consists of six types of protons. The chemical shift of CD protons reported by different authors are very close to those reported in this work. The H-3 and H-5 protons are located in the interior of the CDs cavities and it is, therefore likely that the interaction of the host with the CD inside the cavity will affect the chemical shifts of the H-3 and H-5 protons. A minor shift is observed for the resonance of H-1, H-2 and H-4 located on the exterior of CD. Significant chemical shifts changes Δδ were observed with equimolar mixture of guest and host molecules. Values of pure aldehyde and their (inclusion complexes) are as follows:

2HMB: CHO=10.310 (10.254), OCH_3=3.997 (3.902), OH=6.287 (6.567), 4H=7.990 (7.998), 5H=7.139 (7.312), 6H=8.073 (8.123); **4HMB:** CHO=9.823 (9.578), OCH_3= 3.960 (3.880), OH=6.390 (6.872), 2H=7.422 (7.458), 5H= 7.047 (7.264), 6H=7.428 (7.462); **DMB:** CHO=9.823 (9.523), OCH_3=3.940 (3.911), OCH_3=3.966 (3.879), 2H= 7.422 (7.458), 5H=6.993 (7.031), 6H=7.472 (7.645) and **HDMB:** CHO=9.812 (9.654), OCH_3, OCH_3=3.961 (3.887), OH=6.120 (6.457) and 2H and 6H=7.152 (7.207).

The Δδ values for host protons in the CDs indicate that all the aldehydes are included in the CDs cavities. A significant upfield shift of the CHO and OCH_3 protons confirm that the aldehydes were completely included in the CDs cavities. Further, the well separated signals arising from these benzaldehyde molecules protons in the CD ring suggest that all the benzaldehydes are tightly encapsulated within the CD cavity.

Molecular Modeling of the Inclusion Complexes

A molecular modeling study was performed using PM3 method to find out the most probable conformation of the HMB-CD complex and to give a meaningful 3D visualisation of the inclusion complex. The optimized structure of the aldehydes are shown in Figs. 5, 6 and S3 present the best energy ranked structures of HMB-CD inclusion complexes. The optimized structure, bond distances, bond angles and most out of the ordinary dihedral angles in these molecules before and after complexation considered by PM3 method are presented in Tables S1 and S2. Consistent with the fluorescence results, the molecular modeling studies show that the methoxy/OH group of HMBs is incorporated into the relatively less polar cavity of CDs, while the aldehyde group is present in the upper part of the CDs cavities. The studies also suggest that the probable mode of inclusion of HMB is through its aldehyde group.

Table 5 Binding energies and HOMO, LUMO energy of 2HMB, 4HMB, DMB and HDMB after inclusion complexation by PM3 method

Properties	2HMB α-CD	2HMB - β-CD	4HMB - α-CD	4HMB - β-CD	DMB - α-CD	DMB - β-CD	HDMB - α-CD	HDMB - β-CD
E_{HOMO} (eV)	−8.93	−9.09	−9.51	−8.90	−9.51	−9.13	−9.23	−9.52
E_{LUMO} (eV)	−0.70	−0.52	−0.61	−0.44	−0.68	−0.44	−0.67	−0.94
$E_{HOMO} - E_{LUMO}$ (eV)	−8.23	−8.57	−8.90	−8.46	−8.83	−8.69	−8.56	−8.58
Dipole moment (D)	13.23	9.06	12.42	10.97	8.73	11.35	9.22	8.45
ΔD	0.21	−4.91	−0.16	−2.56	−4.32	−2.65	−4.28	−6.00
E*	−1336.80	−1556.10	−1344.83	−1558.56	−1329.68	−1539.12	−1378.40	−1597.69
ΔE*	−2.16	−7.03	−4.83	−8.45	−0.40	−0.01	−5.63	−14.81
H*	−559.91	−665.80	−567.47	−667.95	−535.28	−638.78	−579.87	−686.01
ΔH*	−9.19	−18.74	−19.70	−23.84	32.45	25.29	−46.84	−56.64
G*	−679.95	−800.97	−686.42	−803.41	−655.91	−776.45	−701.29	−827.07
ΔG*	−10.35	−18.58	−15.24	−19.44	−12.47	−20.22	−30.80	−43.79
S*	−0.392	−0.453	−0.398	−0.454	−0.404	−0.461	−0.407	−0.473
ΔS*	−0.131	−0.136	−0.142	−0.142	−0.150	−0.151	−0.161	−0.171
Zero point energy	728.45	834.43	728.61	834.48	744.96	850.83	748.32	853.69

Unit * = $Kcalmol^{-1}$, ** = cal/mol-Kelvin

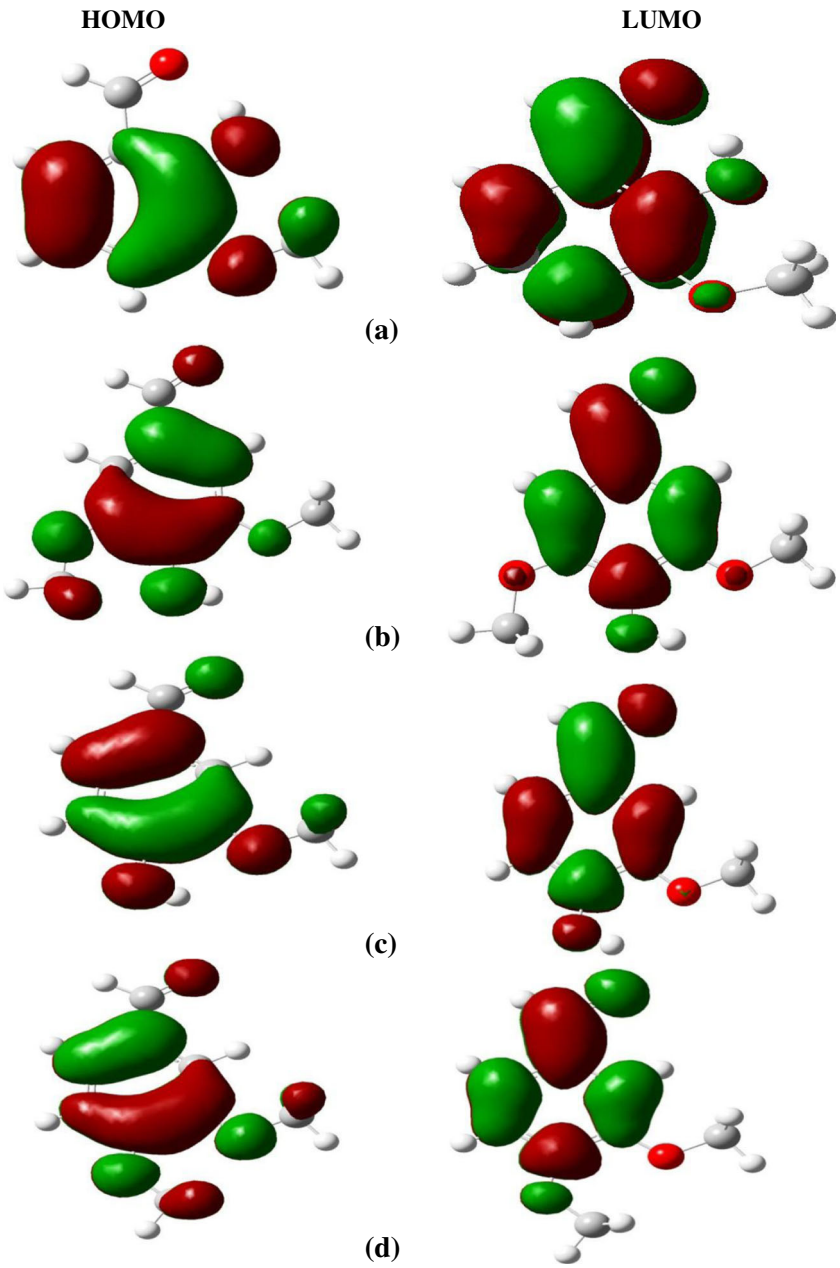

Fig. 7 HOMO-LUMO structure of the inclusion complex **a** 2HMB, **b** 4HMB, **c** DMB and **d** HDMB with β-CD

Tables 4 and 5 shows the calculated binding energy of HMBs complexed with α-CDs and β-CDs. The binding energy change allowed us to evaluate the inclusion process and to find the most stable inclusion complex between the complexes studied. It was evaluated as

$$\Delta E_{complexaton} = E_{complex} - (E_{CD} - E_{HMBs}) \quad (1)$$

where $E_{complex}$, E_{CD} and E_{HMBs} represent the total energy of the complex, the free optimized CDs and the free optimized HMBs respectively. The negative binding energy changes upon complexation clearly demonstrate that CDs can form stable complexes with HMBs. The binding energy change of all the aldehydes with β-CD is more negative than that of α-CD complexes. Also, the binding energy change of HDMB with α-CD/β-CD is more negative than all the other complexes. This indicates that HDMB:α-CD/β-CD forms more stable inclusion complex. It is evidenced that the complexation process is energetically favorable.

The binding energy of the isolated molecules and complexes suggested that stability of the complexes were high compared to isolated molecule. From Tables 4 and 5, the dipole moment of the 2HMB is 1.68 D, 4HMB is 1.24 D, DMB is 1.71 and HDMB is 2.16 D. This was lower than that of the complex, (2HMB:α-CD/β-CD complex ~13.23/9.06 D, 4HMB:α-CD/β-CD complex ~12.42/10.97 D, DMB:α-CD/β-CD complex ~8.73/11.35 D and HDMB:α-CD/β-CD

complex ~9.22/8.45 D lower than the dipole moment for resident molecules. The above quantum mechanical computation values demonstrated a strong relationship with the complexation behavior.

From the optimized structures of the inclusion complexes, one H-bond is formed between 4HMB/α-CD, HDMB with β-CD. The H-bond lengths are shorter than 3.0 Å which just falls within the reported data [39]. This is justified the importance of interaction energy between these molecules and CDs necessary to ensure a better inclusion of the guest to the host. The above values were supported by the fact that the flexibility of the host molecule and substitutions of the guest molecules may be one of the structural requirements for inclusion complexes formation. Further Tables 4 and 5 confirmed that hydrogen bonding interactions also played a major role in the inclusion complexation process.

Frontier Molecular Orbitals

The highest occupied molecular orbitals (HOMOs) and the lowest-lying unoccupied molecular orbitals (LUMOs) are named as frontier molecular orbitals (FMOs). FMOs play in important role in the optical and electric properties, as well as in quantum chemistry and UV–vis spectra [40]. HOMO represents the ability to donate an electron. LUMO as an electron acceptor represents the ability to obtain an electron. The energy gap between HOMO and LUMO determines the kinetic stability, chemical reactivity and optical polarizability and chemical hardness–softness of a molecule [41]. HOMO-LUMO value of 4HMB:α-CD complex is more negative than other inclusion complexes (Fig. 7). This suggests 4HMB:α-CD inclusion complex is more stable than the other inclusion complexes. However, the energy gap between HOMO and LUMO of each complex suggests that these will be no significant change in the electronic spectrum of the guest molecules driving molecular recognition and binding.

Thermodynamics of Inclusion Process

The energetic features, thermodynamic characteristics and electronic properties of these structures were summarized in Tables 4 and 5. The statistical thermodynamic calculations were performed using harmonic frequency analysis in PM3 method for the most stable structures, characterizing them as true minima on the potential energy surface. The frequency analyses were then used for the evaluation of the thermodynamic parameters, such as enthalpy changes (ΔH), entropy contribution (ΔS) and Gibbs free energy (ΔG), for the binding process of HMBs with α-CD and β-CD were summarized in Tables 4 and 5. It can be observed that the inclusion complexation of HMBs with α-CD and β-CD is exothermic judged from the negative enthalpy changes. The enthalpy change for all the HMBs:α-CD/β-CD complexes are more negative than that for the other complexes. It means that all the inclusion processes are enthalpically favorable in nature due to the negative enthalpy changes. The ΔH and ΔS for all the aldehydes with CDs are negative, suggesting that the formation of the inclusion complex is an enthalpy-driven process. Further, a negative ΔG was obtained for all the benzaldehydes imply that the inclusion complexation reaction between these molecules and CDs proceeds spontaneously. Binding of all molecules with CDs is enthalpy-entropy favourable showing negative ΔH and ΔS values.

In Tables S1 and S2, we reported the selected bond distances, bond angles and the most interesting angles between the hydroxyl group and phenyl ring of these aldehydes before and after complexation for the most stable inclusion complex. From comparison of free guest and the complex, it is clear that the geometrical structures of the aldehydes after complexation are completely altered. This alteration is achieved through the variation of the dihedral angles between the phenyl ring and the alkyl chain of these drugs which is subject to a distortion to adopt a specific conformation leading to the formation of a most stable complex. The non-bonded interaction between the phenyl ring and CD might be responsible for the difference in structure/stability of the complex. Experimental thermodynamic values will be helpful for numerical investigations in order to draw a conclusion about the effect of solvent on the binding of complexation.

Conclusion

The inclusion complexes of α-CD, β-CD, HP-α-CD and HP-β-CD with four aldehydes (2HMB, 4HMB, DMB and HDMB) were investigated by UV–Vis, steady-state and time-resolved fluorescence and molecular modeling techniques. Dual fluorescence observed in solvents and the CD mediums are responsible for intramolecular charge transfer effect in all the aldehydess. The spectral data of all the benzaldehydes in the CDs clearly demonstrate the formations of 1:1 inclusion complexes were formed. The PM3 results suggest that the complexation of HDMB/α-CD and β-CD are significantly more favorable than the other complexes. The results confirmed aromatic ring for each compound is totally embedded in CDs cavities. The statistical thermodynamic calculations suggest that formation of the inclusion complexes is enthalpy driven process.

Acknowledgements This work is supported by the CSIR [No. 01(2549)/12/EMR-II], and UGC [F.No. 41-351/2012 (SR)]. The authors thank to Dr. P. Ramamurthy, Director, National centre for ultrafast processes, Madras University for allowing the fluorescence lifetime measurements available for this work.

References

1. Szejtli J (1998) Chem Rev 98:1743–1754
2. Connors KA (1997) Chem Rev 97:1325–1357
3. Breslow R, Dong SD (1998) Chem Rev 98:1997–2011
4. Lipkowits KB (1998) Chem Rev 98:1829–1873
5. Guo QX, Liu L, Cai WS, Jiang Y, Liu YC (1998) Chem Phys Lett 290:514–518
6. Liu L, Guo QX (1999) J Phys Chem B 103:3461–3467
7. Lu TX, Zhang DP, Dong SJ (1990) Acta Chimca Sinica 48:1071–1074
8. Alvira E, Mayoral JA, Gareia JI (1997) Chem Phys Lett 271:178–184
9. Guo QX, Liu HY, Ruan XQ, Zheng XQ, Shi YY, Liu YC (1999) J Inclu Phenom 35:487–496
10. Dodziuk H, Lukin O, Nowinski KS (2000) J Mol Structure (THEOCHEM) 503:221–230
11. Li XS, Liu L, Guo QX, Chu SD, Liu YC (1999) Chem Phys Lett 307: 117–120
12. Liu L, Li XS, Guo QX, Liu YC (1999) Chin Chem Lett 10:1053–1056
13. Song KS, Liu L, Li XS, Guo QX (2000) Res Chem Intermed 26:319–325
14. Loftsson T, Duchene D (2007) Int J Pharm 329:1–11
15. De Lisi R, Lazzara G (2009) Therm Anal Calorim 97:797–803
16. Novak CS, Ehen Z, Fodor M, Jiesinszky L, Orgovanyi J (2006) J Therm Anal Calorim 84:693–701
17. Stalin T, Rajendiran N (2005) Spectrochim Acta, A 61A:3087–3096
18. Rajendiran N, Balasunbramanian T (2008) Spectrochim Acta A 69: 822–829
19. Stalin T, Sivakumar G, Shanthi B, Sekar A, Rajendiran N (2006) J Photochem Photobiol A: Chemistry 177:144–155
20. Stalin T, Rajendiran N (2006) J Molecular Structure 794:35–45
21. Siva S, Sankaranarayanan RK, Prabhu AAM, Rajendiran N (2009) Indian J Chemistry 48A:1515–1521
22. Sankaranarayanan RK, Siva S, Prabhu AAM, Rajendiran N (2010) J Incl Phenom Macrocycl Chem 67:461–470
23. Jorgenson MJ, Hartter DR (1963) J Am Chem Soc 85:878–883
24. Yagil G (1967) J Phys Chem 71:1034–1038
25. Yan C, Li X, Xiu Z, Hao C (2006) J Mol Struct: THEOCHEM 764: 95–100
26. Sayede AD, Ponchel A, Filardo G, Galia AE, Monflier E (2006) J Mol Struct: THEOCHEM 777:99–106
27. Al-Souod KA (2006) J Inclus Phenom Macrocyclic Chem 54:123–127
28. Seridi L, Boufelfel A (2011) J Mol Liq 158:151–158
29. Dearden JC, Forbes WF (1958) Can J Chem 23:1362–1370
30. Benesi HA, Hildebrand JH (1949) J Am Chem Soc 71:2703–2707
31. Prabhu AAM, Sankaranarayanan RK, Siva S, Rajendiran N (2009) Spectrochim Acta A 74:484–497
32. Smith AA, Kannan K, Manavalan R, Rajendiran R (2010) J Fluores 20:809–820
33. Prabhu AAM, Sankaranarayanan RK, Venkatesh G, Rajendiran N (2012) J Phys Chem B 116:9061–9074
34. Prabhu AAM, Rajendiran N (2012) J Fluores 22:1461–1474
35. Rajendiran N, Swaminathan M (1996) Ind J Chem 35A:818–824
36. Rajendiran N, Swaminathan M (1997) Int J Chem Kinetics 29:861–867
37. Bangal PR, Panja S, Chakravorti S (2001) J Photochem Photobiol A Chem 139:5–16
38. Panja S, Bangal PR, Chakravorty S (2000) Chem Phys Lett 329:377–385
39. Senger M, in Atwood JL, Davies JED & Macnicol DD (Eds) (1984) Inclusion complexes, Vol. II. Academic press, London, pp 231–290
40. Asiri AM, Karabacak M, Kurt M, Alamry KA (2011) Spectrochim Acta A 82:444–455
41. Kosar B, Albayrak C (2011) Spectrochim Acta A 78:160–167